

Promises and Caveats of Uplink IoT Ultra-Dense Networks

Ming Ding[‡], David López Pérez[†]

[‡]Data61, Australia {Ming.Ding@data61.csiro.au}

[†]Nokia Bell Labs, Ireland {david.lopez-perez@nokia.com}

Abstract—In this paper, by means of simulations, we evaluate the uplink (UL) performance of an Internet of Things (IoT) capable ultra-dense network (UDN) in terms of the coverage probability and the density of reliably working user equipments (UEs). From our study, we show the benefits and challenges that UL IoT UDNs will bring about in the future. In more detail, for a low-reliability criterion, such as achieving a UL signal-to-interference-plus-noise ratio (SINR) above 0 dB, the density of reliably working UEs grows quickly with the network densification, showing the potential of UL IoT UDNs. In contrast, for a high-reliability criterion, such as achieving a UL SINR above 10 dB, the density of reliably working UEs remains to be low in UDNs due to excessive inter-cell interference, which should be considered when operating UL IoT UDNs. Moreover, considering the existence of a non-zero antenna height difference between base stations (BSs) and UEs, the density of reliably working UEs could even *decrease* as we deploy more BSs. This calls for the usage of sophisticated interference management schemes and/or beam steering/shaping technologies in UL IoT UDNs.

I. INTRODUCTION

Recent years have seen rapid advancement in the development and deployment of Internet of Things (IoT) networks, which can be attributed to the increasing communication and sensing capabilities combined with the falling prices of IoT devices [1]. For example, base stations (BSs) can be equipped with the latest IoT technologies, such as the new generation of machine type communications [2], to collect data from gas, water, and power meters via uplink (UL) transmissions. In practice, such BSs can take the form of both terrestrial and aerial ones [3].

This poses, however, a challenge to the wireless industry, which must offer an increasing volume of reliable traffic in a profitable and energy efficient manner, especially for the UL communications. In this context, the orthogonal deployment of ultra-dense (UD) small cell networks (SCNs), or simply ultra-dense networks (UDNs), have been selected as one of the workhorse for network enhancement in the fourth-generation (4G) and fifth-generation (5G) networks developed by the 3rd Generation Partnership Project (3GPP) [2]. Here, orthogonal deployment means that UDNs and macrocell networks operate on different frequency spectrum, which simplifies network management due to no inter-tier interference.

The performance analysis of IoT UDNs is, however, particularly challenging for the UL because *i)* UDNs are fundamentally different from the current sparse/dense networks [4] and *ii)* the UL power control mechanism operates according

to the random user equipment (UE) positions in the network, which is quite different from the constant power setting in the downlink (DL) [5].

In this paper, by means of simulations, we evaluate the network performance of UL IoT UDNs in terms of the coverage probability and the density of reliably working UEs. The main findings of this paper are as follows:

- We find that for a low-reliability criterion, such as achieving a UL signal-to-interference-plus-noise ratio (SINR) above $\gamma = 0$ dB, the density of reliably working UEs quickly grows with the network densification, showing the benefits of UL IoT UDNs. In contrast, for a high-reliability criterion, such as achieving a UL SINR above $\gamma = 10$ dB, the density of reliably working UEs remains low in UDNs due to excessive inter-cell interference, which should be considered when operating UL IoT UDNs.
- We find that due to the existence of a non-zero antenna height difference between BSs and UEs, the density of reliably working UEs could even *decrease* as we deploy more BSs in a UL IoT UDN. This calls for the usage of sophisticated interference management schemes and/or beam steering/shaping technologies in UL IoT UDNs.
- We find that the correlated shadow fading allows a BS with a lower environmental fading factor to provide connection to a larger number of UEs. Thus, its theoretical analysis is an open problem for further study.
- We find that the optimized hexagonal-like BS deployment can improve network performance for relatively sparse networks, but not for UDNs. Thus, its theoretical study is not urgent.

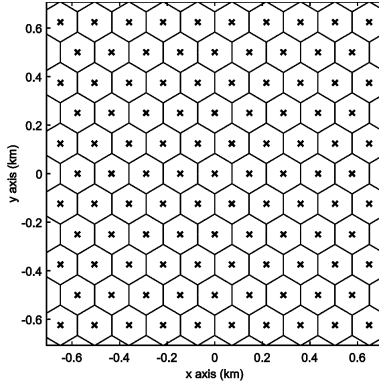
II. DISCUSSION ON THE ASSUMPTIONS OF UL IoT UDNs

In this section, we discuss several important assumptions in UL IoT UDNs.

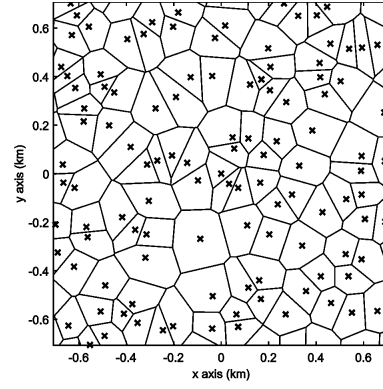
A. BS Deployments

In general, to study the performance of a UL IoT network, two types of BS deployments can be found in the literature, i.e., the hexagonal and the random deployments as shown in Fig. 1.

In Fig. 1, BSs are represented by markers “x” and cell coverage areas are outlined by solid lines. Note that the hexagonal BS deployment leads to an upper-bound performance because BSs are evenly distributed in the network scenario,



(a) The hexagonal BS deployment.



(b) The random BS deployment.

Fig. 1: Illustration of two widely accepted types of BS deployments. Here, BSs are represented by markers “x” and cell coverage areas for user equipment (UE) distribution are outlined by solid lines.

and thus very strong interference due to close BS proximity is precluded [6]. In contrast, the random BS deployment reflects a more realistic network deployment with more challenging interference conditions [2, 7]. For completeness, in our following performance evaluation, we will consider both BS deployments.

B. Antenna Heights

In the performance analysis of the conventional sparse or dense cellular networks, the antenna height difference between BSs and UEs is usually ignored due to the dominance of the horizontal distance. However, with a much shorter distance between a BS and its served UEs in an UDN, such antenna height difference becomes non-negligible [7]. The performance impact of such antenna height difference between BSs and UEs on the DL UDNs has been investigated in [8]. More specifically, the existence of a non-zero antenna height difference between BSs and UEs gives rise to a non-zero cap on the minimum distance between a BS and its served UEs, and thus *a cap on the received signal power strength*. Thus, and although each inter-cell interference power strength is subject to the same cap, the aggregate inter-cell interference power will overwhelm the signal power in an UDN due to the sheer number of strong interferers. Consequently, the antenna height difference between BSs and UEs should be considered in the performance evaluation of UL IoT UDNs.

C. Line-of-Sight Transmissions

A much shorter distance between a BS and its served UEs in an UDN implies a higher probability of line-of-sight (LoS) transmissions. The performance impact of such LoS transmissions on the DL of UDNs has been shown to be significant in [9, 10]. Generally speaking, LoS transmissions are more helpful to enhance the received signal strength than non-line-of-sight (NLoS) transmissions. However, after a certain level of BS densification, not only the signal power, but also the inter-cell interference power will significantly grow due to *the emergence of LoS interfering paths*. Thus, the transition of a large number of interfering paths from

NLoS to LoS will overwhelm the signal power in an UDN. Consequently, the probabilistic LoS transmissions should also be considered in the performance evaluation of UL IoT UDNs.

D. BS Idle Mode

Considering the surplus of BSs in UDNs, a BS can be put to sleep when there is no active UE connected to it, which is referred as the BS idle mode capability (IMC) [11, 12]. As a result, the active UEs’ SINR can benefit from *i)* a BS selection diversity gain, i.e., each UE has a plurality of BSs to select its server from, and *ii)* a tight control of inter-cell interference, as effective UL inter-cell interference only comes from active UEs served by active neighboring BSs. The surplus of BSs together with the IMC can be seen as a powerful tool that can mitigate the interference problems presented in the previous subsections. However, it should be noted that switching off BSs has a negative impact on the number of IoT UEs that can concurrently transmit.

III. SYSTEM MODEL

For a certain time-frequency resource block (RB), we consider a UL IoT network with BSs deployed on a plane according to the hexagonal deployment or the random deployment, as shown in Fig. 1. For both BS deployments, the density of BSs is denoted by λ BSs/km². Furthermore, we consider a homogeneous Poisson point process (HPPP) Φ to characterize the random deployment.

Active UEs are assumed to be distributed following an HPPP with a density of ρ UEs/km². Here, we only consider active UEs in the network because non-active UEs do not trigger data transmission. Note that the total number of UEs, e.g., phones, gateways, sensors, tags, etc., in a UL IoT network should be much higher than the number of the active UEs. However, we believe that in a certain time-frequency RB, the active UEs with non-zero data traffic demands should still be not many. For example, a typical density of active UEs is around 300 UEs/km² in 5G [2].

A. Channel Model

The two-dimensional (2D) distance between a BS and a UE is denoted by r . Moreover, the absolute antenna height difference between a BS and a UE is denoted by L . Thus, the 3D distance between a BS and a UE can be expressed as

$$w = \sqrt{r^2 + L^2}. \quad (1)$$

Note that the value of L is in the order of several meters [13].

Following [10], we adopt a general path loss model, where the path loss $\zeta(w)$ is a multi-piece function of w written as

$$\zeta(w) = \begin{cases} \zeta_1(w), & \text{when } L \leq w \leq d_1 \\ \zeta_2(w), & \text{when } d_1 < w \leq d_2 \\ \vdots & \vdots \\ \zeta_N(w), & \text{when } w > d_{N-1} \end{cases}, \quad (2)$$

where each piece $\zeta_n(w)$, $n \in \{1, 2, \dots, N\}$ is modeled as

$$\zeta_n(w) = \begin{cases} \zeta_n^L(w) = A_n^L w^{-\alpha_n^L}, & \text{LoS: } \Pr_n^L(w) \\ \zeta_n^{\text{NL}}(w) = A_n^{\text{NL}} w^{-\alpha_n^{\text{NL}}}, & \text{NLoS: } 1 - \Pr_n^L(w) \end{cases}, \quad (3)$$

where

- $\zeta_n^L(w)$ and $\zeta_n^{\text{NL}}(w)$, $n \in \{1, 2, \dots, N\}$ are the n -th piece path loss functions for the LoS and the NLoS cases, respectively,
- A_n^L and A_n^{NL} are the path losses at a reference 3D distance $w = 1$ for the LoS and the NLoS cases, respectively,
- α_n^L and α_n^{NL} are the path loss exponents for the LoS and the NLoS cases, respectively, and
- $\Pr_n^L(w)$ is the n -th piece LoS probability function that a transmitter and a receiver separated by a 3D distance w has an LoS path, which is assumed to be a *monotonically decreasing function* with respect to w . Existing measurement studies have confirmed this assumption [13].

Moreover, we assume that each BS/UE is equipped with an isotropic antenna, and that the multi-path fading between a BS and a UE is independently identical distributed (i.i.d.) Rayleigh distributed [9, 10, 14].

B. User Association Strategy

We assume a practical user association strategy (UAS), in which each UE is connected to the BS giving the maximum average received signal strength [10, 14]. Such UAS can be formulated by

$$b_o = \arg \max_b \{ \bar{R}_b(w) \}, \quad (4)$$

where $\bar{R}_b(w)$ denotes the average received signal strength from BS b and the UE of interest, separated by a distance of w . Assuming a constant BS transmission power, $\bar{R}_b(w)$ can be equivalently evaluated by $\zeta(w)$ defined in (2).

As a special case to show our numerical results in the simulation section, we consider a practical two-piece path loss function and a two-piece exponential LoS probability function, defined by the 3GPP [13]. More specifically, in (2) we use $N = 2$, $\zeta_1^L(w) = \zeta_2^L(w) = A^L w^{-\alpha^L}$, $\zeta_1^{\text{NL}}(w) =$

$\zeta_2^{\text{NL}}(w) = A^{\text{NL}} w^{-\alpha^{\text{NL}}}$, $\Pr_1^L(w) = 1 - 5 \exp(-R_1/w)$, and $\Pr_2^L(w) = 5 \exp(-w/R_2)$, where $R_1 = 156$ m, $R_2 = 30$ m, and $d_1 = \frac{R_1}{\ln 10} = 67.75$ m [13]. For clarity, this path loss case is referred to as **the 3GPP Case** hereafter.

C. BS Activation Model

As discussed in Subsection II-D, a BS will enter an idle mode if there is no UE connected to it. Thus, the set of active BSs is determined by the UAS. Since UEs are randomly and uniformly distributed in the network and given the adopted UAS strategy, we can assume that the active BSs also follow an HPPP distribution $\tilde{\Phi}$ [11], the density of which is denoted by $\tilde{\lambda}$ BSs/km², where $\tilde{\lambda} \leq \lambda$ and $\tilde{\lambda} \leq \rho$. Note that $\tilde{\lambda}$ also characterizes the density of active UEs because no collision exists in the centralized cellular IoT UDNs.

For illustration purposes, considering a single-slope path loss model and a nearest-BS UAS, $\tilde{\lambda}$ can be calculated as [11]

$$\tilde{\lambda} = \lambda \left[1 - \frac{1}{\left(1 + \frac{\rho}{q\lambda}\right)^q} \right], \quad (5)$$

where an empirical value of 3.5 was suggested for q in [11]¹.

D. UL Power Control Model

The UE power, denoted by P^{UE} , is subject to semi-static power control (PC) in practice. In this paper, we adopt the fractional path loss compensation (FPC) scheme standardized in 4G [13], which can be modeled as

$$P^{\text{UE}} = 10^{\frac{P_0}{10}} [\zeta(w)]^{-\eta} N^{\text{RB}}, \quad (6)$$

where P_0 is the target received power in dBm on each RB at the BS, $\eta \in (0, 1]$ is the FPC compensation factor, and N^{RB} is the number of RBs in the frequency domain.

E. The Coverage Probability

Based on this system model, we can define the coverage probability that the typical UE's UL SINR is above a designated threshold γ as

$$p^{\text{cov}}(\lambda, \gamma) = \Pr[\text{SINR}^{\text{U}} > \gamma], \quad (7)$$

where the UL SINR is calculated by

$$\text{SINR}^{\text{U}} = \frac{P_{b_o}^{\text{UE}} \zeta(w_{b_o}) h}{I_{\text{agg}}^{\text{U}} + P_{\text{N}}^{\text{U}}}, \quad (8)$$

where b_o denotes the serving BS of the typical UE, $P_{b_o}^{\text{UE}}$ is the UE transmission power given by (6), w_{b_o} is the distance from the typical UE to its serving BS b_o , h is the Rayleigh channel gain modeled as an exponentially distributed random variable (RV) with a mean of one as mentioned above, P_{N}^{U} is the additive white Gaussian noise (AWGN) power at the serving BS b_o , and $I_{\text{agg}}^{\text{U}}$ is the UL aggregate interference.

¹Note that according to [12], q should also depend on the path loss model with LoS/NLoS transmissions. Having said that, [12] also showed that (5) is generally very accurate to characterize $\tilde{\lambda}$ for the 3GPP Case with LoS/NLoS transmissions.

F. The Density of Reliably Working UEs

Based on the definitions of the active BS density in Subsection III-C and the coverage probability in Subsection III-E, we can further define a density of reliably working UEs that can operate above a target UL SINR threshold γ as

$$\tilde{\rho} = \tilde{\lambda} p^{\text{cov}}(\lambda, \gamma), \quad (9)$$

where the active BS density $\tilde{\lambda}$ measures the maximum density of UEs that can simultaneously transmit, and the coverage probability $p^{\text{cov}}(\lambda, \gamma)$ scales down $\tilde{\lambda}$, giving the density of reliably working UEs. The larger the UL SINR threshold γ , the higher the reliability of the IoT communications, and thus the less the UEs that can simultaneously achieve such reliability.

G. More Refined Assumptions

In performance analysis, the multi-path fading is usually modeled as Rayleigh fading for simplicity. However, in the 3GPP, a more practical model based on generalized Rician fading is widely adopted for LoS transmissions [15]. In such model, the K factor in dB scale (the ratio between the power in the direct path and the power in the other scattered paths) is modeled as $K[\text{dB}] = 13 - 0.03w$, where w is defined in (1). More specifically, let h^L denote the multi-path fading power for LoS transmissions. Then, for the 3GPP model of Rician fading, h^L follows a non-central chi-squared distribution with its PDF given by [16]

$$f(h^L) = (K+1) \exp(-K - (K+1)h^L) \times I_0\left(2\sqrt{K(K+1)h^L}\right), \quad (10)$$

where K is the distance-dependent value discussed above and $I_0(\cdot)$ is the 0-th order modified Bessel function of the first kind [16].

Moreover, the shadow fading is also usually not considered or simply modeled as i.i.d. RVs in performance analysis. However, in the 3GPP, a more practical correlated shadow fading is often used [13, 15, 17], where the shadow fading in dB unit is modeled as zero-mean Gaussian RV [13]. More specifically, the shadow fading coefficient in dB unit between BS b and UE u is formulated as [13]

$$S_{bu} = \sqrt{\tau} S_u^{\text{UE}} + \sqrt{1-\tau} S_b^{\text{BS}}, \quad (11)$$

where τ is the correlation coefficient of shadow fading, S_u^{UE} and S_b^{BS} are i.i.d. zero-mean Gaussian RVs attributable to UE u and BS b , respectively. The variance of S_u^{UE} and S_b^{BS} is denoted by σ_{Shad}^2 . In [13], it is suggested that $\tau = 0.5$ and $\sigma_{\text{Shad}} = 10$ dB.

Considering the distance-dependent Rician fading for LoS transmissions and the correlated shadow fading, we can upgrade the 3GPP Case to an advanced 3GPP Case. In the next section, we will present simulation results of UL IoT UDNs for both the 3GPP Case and the **Advanced 3GPP Case**. It should be noted that for the Advanced 3GPP Case, shadow fading should be considered in the computation of $\bar{R}_b(w)$, i.e., $\bar{R}_b(w)$ should be evaluated by $\zeta(w) \times 10^{\frac{S_{bu}}{10}}$ in (4).

IV. SIMULATION AND DISCUSSION

In this section, we present numerical results to validate the accuracy of our analysis. According to Tables A.1-3~A.1-7 of [13], we adopt the following parameters for the 3GPP Case: $\alpha^L = 2.09$, $\alpha^{\text{NL}} = 3.75$, $A^L = 10^{-10.38}$, $A^{\text{NL}} = 10^{-14.54}$, $P_0 = -76$ dBm, $\eta = 0.8$, $N^{\text{RB}} = 55$, $P_N = -91$ dBm (with a noise figure of 13 dB), $\tau = 0.5$ and $\sigma_{\text{Shad}} = 10$ dB.

A. Performance Results of the 3GPP Case

In Figs. 2 and 3, we plot the performance results of the 3GPP Case for $\gamma = 0$ dB and $\gamma = 10$ dB, respectively. Here, we only consider realistic networks with the random deployment of BSs. From these two figures, we can draw the following observations:

- Figs. 2a and 3a show that the active BS density $\tilde{\lambda}$ monotonically increases with the network densification, and it is bounded by $\rho = 300$ UEs/km². Such results are in line with the analytical results in (5) [11, 12]. However, the density of reliably working UEs $\tilde{\rho}$, i.e., $\tilde{\lambda} p^{\text{cov}}(\lambda, \gamma)$ defined in (9), does not necessarily grow as the BS density λ increases. This is because $p^{\text{cov}}(\lambda, \gamma)$ is a non-monotone function with respect to λ , which will be explained in the following.
- When the BS density λ is around $\lambda \in [10^{-1}, 70]$ BSs/km², the network is noise-limited, and thus $p^{\text{cov}}(\lambda, \gamma)$ increases with λ as the network is lightened up with coverage and the signal power strength benefits from LoS transmissions.
- When the BS density λ is around $\lambda \in [70, 400]$ BSs/km², $p^{\text{cov}}(\lambda, \gamma)$ decreases with λ . This is due to the transition of a large number of interfering paths from NLoS to LoS, which accelerates the growth of the aggregate inter-cell interference. Such performance behavior has been reported in [10] for the DL and [18] for the UL.
- When $\lambda \in [400, 10^4]$ BSs/km², $p^{\text{cov}}(\lambda, \gamma)$ continuously increases thanks to the BS IMC [12], i.e., the signal power continues increasing with the network densification due to the BS diversity gain, while the aggregate interference power becomes constant, as $\tilde{\lambda}$ is bounded by ρ . However, as shown in Figs. 2b and 3b, the antenna height difference L between BSs and UEs has a large impact on $p^{\text{cov}}(\lambda, \gamma)$ because a non-zero L places a bound on the signal power strength, which degrades the coverage performance. In more detail, when $\lambda = 10^4$ BSs/km² and $\gamma = 0$ dB, the coverage probability with $L = 8.5$ m loses 13 % compared to that with $L = 0$ m. Such performance degradation further enlarges to 32 % when $\lambda = 10^4$ BSs/km² and $\gamma = 10$ dB, showing a much less chance of UE working reliably above 10 dB.
- Due to the complicated performance behavior of $p^{\text{cov}}(\lambda, \gamma)$, the density of reliably working UEs $\tilde{\rho}$ displayed in Figs. 2c and 3c depends on the following factors:
 - For a low-reliability criterion, such as surpassing a UL SINR threshold of $\gamma = 0$ dB, the density of reliably working UEs $\tilde{\rho}$ grows quickly with the network

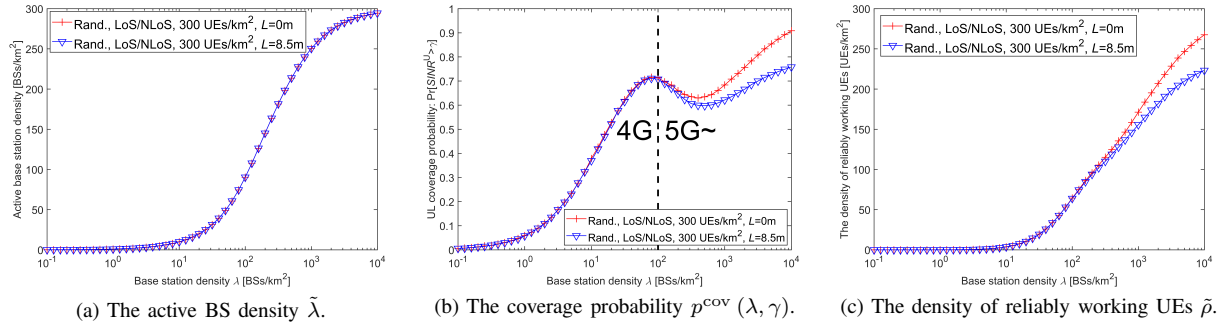


Fig. 2: Performance results of the 3GPP Case (Rayleigh fading, no shadow fading) with $\gamma = 0$ dB.

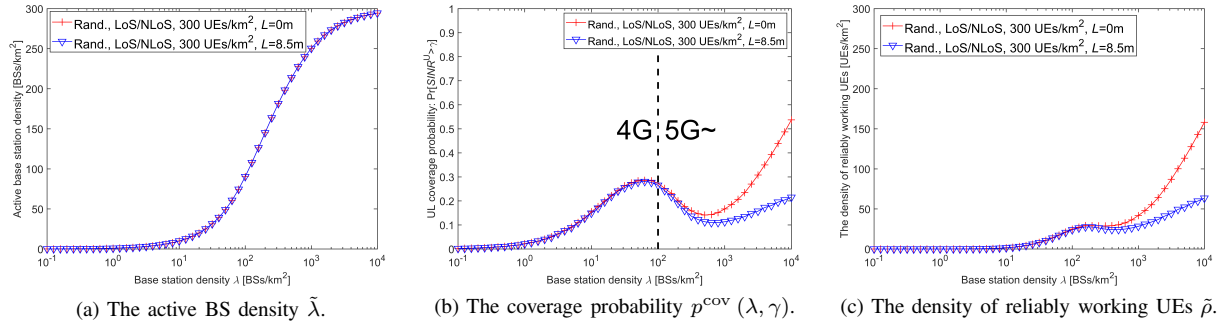


Fig. 3: Performance results of the 3GPP Case (Rayleigh fading, no shadow fading) with $\gamma = 10$ dB.

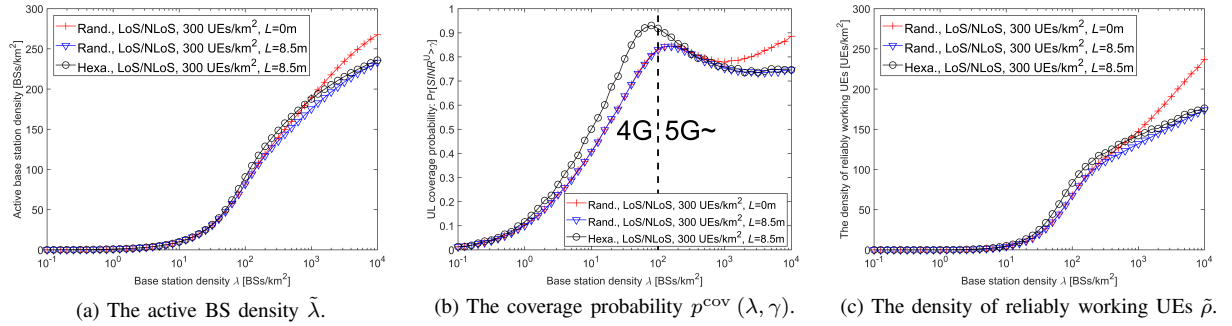


Fig. 4: Performance results of the Advanced 3GPP Case (Rician fading for LoS, correlated shadow fading) with $\gamma = 0$ dB.

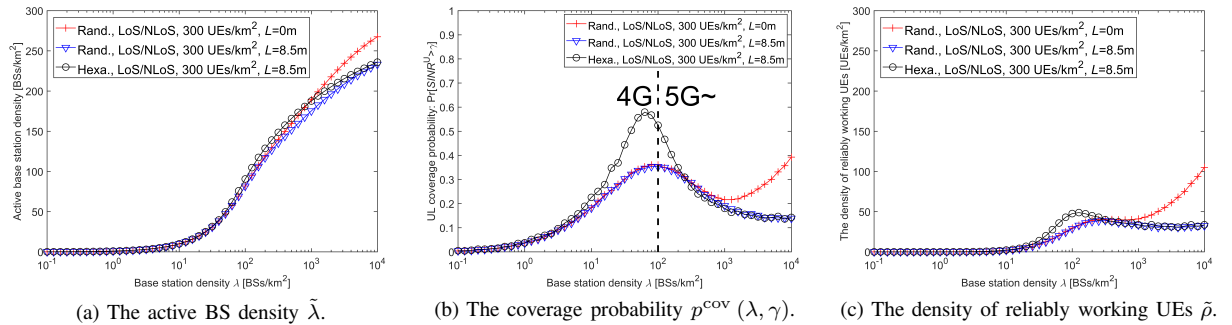


Fig. 5: Performance results of the Advanced 3GPP Case (Rician fading for LoS, correlated shadow fading) with $\gamma = 10$ dB.

densification, showing the benefits of UL IoT UDNs. In contrast, for a high-reliability criterion, such as surpassing a UL SINR threshold of $\gamma = 10$ dB, the density of reliably working UEs $\tilde{\rho}$ does not exhibit a satisfactory performance even in UDNs, e.g., we merely get $\tilde{\rho} < 50$ UEs/km² when $\lambda = 10^3$ BSs/km². The situation only improves when the BS IMC fully kicks in, e.g., $\lambda > 10^3$ BSs/km².

- Considering the existence of a non-zero L , the density of reliably working UEs $\tilde{\rho}$ could even *decrease* as we deploy more BSs (see Fig. 3c, $\lambda \in [200, 600]$ BSs/km²). This calls for the usage of sophisticated interference management schemes [19] in UL IoT UDNs. Another solution to mitigate such strong inter-cell interference is beam steering/shaping using multi-antenna technologies [2].

B. Performance Results of the Advanced 3GPP Case

In Figs. 4 and 5, we plot the performance results of the Advanced 3GPP Case for $\gamma = 0$ dB and $\gamma = 10$ dB, respectively. To make our study more complete, here we consider both the random and the hexagonal deployments of BSs. From these two figures, we can see that the previous conclusions are qualitatively correct, which indicates that it is not urgent to investigate Rician fading and/or correlated shadow fading in the context of UDNs. However, there are two new observations that are worth mentioning:

- From Figs. 2a/3a and Figs 4a/5a, we can see that the active BS density $\tilde{\lambda}$ of the Advanced 3GPP Case is smaller than that of the 3GPP Case. This means that (5) is no longer accurate to characterize $\tilde{\lambda}$ for the Advanced 3GPP Case. This is because the correlated shadow fading allows a BS with a lower environmental fading factor, i.e., S_b^{BS} , to attract more UEs than other BSs with higher values of S_b^{BS} . Its theoretical analysis is an open problem for further study.
- The hexagonal deployment of BSs can improve network performance for relatively sparse networks (e.g., $\lambda < 10^2$ BSs/km²), but not for UDNs (e.g., $\lambda > 10^3$ BSs/km²). Such conclusion indicates that it is not urgent to investigate the performance of UDNs with the hexagonal deployment of BSs, which has been a long-standing open problem for decades [5].

V. CONCLUSION

We presented simulation results to evaluate the network performance of UL IoT UDNs. From our study, we can see that for a low-reliability criterion, the density of reliably working UEs grows quickly with the network densification. However, in our journey to realize a more reliable UL IoT UDNs, we should be aware of several caveats:

- First, for a high-reliability criterion, the density of reliably working UEs remains low in UDNs due to excessive inter-cell interference, which should be considered when operating UL IoT UDNs.

- Second, due to the existence of a non-zero antenna height difference between BSs and UEs, the density of reliably working UEs could even *decrease* as we deploy more BSs. This calls for further study of UL IoT UDNs.
- Third, well-planned hexagonal-like BS deployments can improve network performance for relatively sparse networks, but not for UDNs, showing that alternative solutions other than BS position optimization should be considered in the future UL IoT UDNs.

REFERENCES

- [1] A. Al-Fuqaha, M. Guizani, M. Mohammadi, M. Aledhari, and M. Ayyash, "Internet of things: A survey on enabling technologies, protocols, and applications," *IEEE Communications Surveys Tutorials*, vol. 17, no. 4, pp. 2347–2376, Fourthquarter 2015.
- [2] D. López-Pérez, M. Ding, H. Claussen, and A. Jafari, "Towards 1 Gbps/UE in cellular systems: Understanding ultra-dense small cell deployments," *IEEE Communications Surveys Tutorials*, vol. 17, no. 4, pp. 2078–2101, Jun. 2015.
- [3] A. Fotouhi, M. Ding, and M. Hassan, "Understanding autonomous drone maneuverability for Internet of Things applications," pp. 1–6, Jun. 2017.
- [4] M. Ding, D. López-Pérez, H. Claussen, and M. A. Kâafar, "On the fundamental characteristics of ultra-dense small cell networks," to appear in *IEEE Network Magazine*, arXiv:1710.05297 [cs.IT], Oct. 2017. [Online]. Available: <http://arxiv.org/abs/1710.05297>
- [5] M. Ding, D. López-Pérez, G. Mao, and Z. Lin, "Microscopic analysis of the uplink interference in FDMA small cell networks," *IEEE Trans. on Wireless Communications*, vol. 15, no. 6, pp. 4277–4291, Jun. 2016.
- [6] J. Andrews, F. Baccelli, and R. Ganti, "A tractable approach to coverage and rate in cellular networks," *IEEE Transactions on Communications*, vol. 59, no. 11, pp. 3122–3134, Nov. 2011.
- [7] 3GPP, "TR 36.872: Small cell enhancements for E-UTRA and E-UTRAN - Physical layer aspects," Dec. 2013.
- [8] M. Ding and López-Pérez, "Performance impact of base station antenna heights in dense cellular networks," to appear in *IEEE Transactions on Wireless Communications*, arXiv:1704.05125 [cs.NI], Sep. 2017. [Online]. Available: <https://arxiv.org/abs/1704.05125>
- [9] X. Zhang and J. Andrews, "Downlink cellular network analysis with multi-slope path loss models," *IEEE Transactions on Communications*, vol. 63, no. 5, pp. 1881–1894, May 2015.
- [10] M. Ding, P. Wang, D. López-Pérez, G. Mao, and Z. Lin, "Performance impact of LoS and NLoS transmissions in dense cellular networks," *IEEE Transactions on Wireless Communications*, vol. 15, no. 3, pp. 2365–2380, Mar. 2016.
- [11] S. Lee and K. Huang, "Coverage and economy of cellular networks with many base stations," *IEEE Communications Letters*, vol. 16, no. 7, pp. 1038–1040, Jul. 2012.
- [12] M. Ding, D. López-Pérez, G. Mao, and Z. Lin, "Performance impact of idle mode capability on dense small cell networks with LoS and NLoS transmissions," to appear in *IEEE Transactions on Vehicular Technology*, arXiv:1609.07710 [cs.NI], Sep. 2017.
- [13] 3GPP, "TR 36.828: Further enhancements to LTE Time Division Duplex for Downlink-Uplink interference management and traffic adaptation," Jun. 2012.
- [14] T. Bai and R. Heath, "Coverage and rate analysis for millimeter-wave cellular networks," *IEEE Transactions on Wireless Communications*, vol. 14, no. 2, pp. 1100–1114, Feb. 2015.
- [15] Spatial Channel Model AHG, "Subsection 3.5.3, Spatial Channel Model Text Description V6.0," Apr. 2003.
- [16] I. Gradshteyn and I. Ryzhik, *Table of Integrals, Series, and Products (7th Ed.)*. Academic Press, 2007.
- [17] M. Ding, M. Zhang, D. López-Pérez, and H. Claussen, "Correlated shadow fading for cellular network system-level simulations with wrap-around," *2015 IEEE International Conference on Communications (ICC)*, pp. 2245–2250, Jun. 2015.
- [18] T. Ding, M. Ding, G. Mao, Z. Lin, D. López-Pérez, and A. Y. Zomaya, "Uplink performance analysis of dense cellular networks with LoS and NLoS transmissions," *IEEE Transactions on Wireless Communications*, vol. 16, no. 4, pp. 2601–2613, Apr. 2017.
- [19] M. Ding and H. Luo, *Multi-point Cooperative Communication Systems: Theory and Applications*. Springer, 2013.